Tristate Converters

FELIX A. HIMMELSTOSS
Faculty of Electronic Engineering and Entrepreneurship,
University of Applied Sciences Technikum Wien,
Hoechstaedtplatz 6, 1200 Vienna,
AUSTRIA

Abstract: - In the continuous inductor current operation the tristate DC/DC converters have three modes. In the first mode, the active switches are on and energy is transferred into the coil. In the second mode, the coil is short-circuited and the current in the coils stays constant, and in the third mode, the free-wheeling diode takes over the current. In the here used concept the active switch of the original converter is replaced by a series connection of two active switches and an additional diode is connected to the connection point of the two electronic switches. The other terminal of the diode is connected to the coil. This concept was originally applied to the Boost converter. In this paper, it is shown that the same idea can be applied to other DC/DC converters and the Buck and the Buck-Boost converters are shown. It is also possible to apply the concept to converters of higher order. Here the Cuk, Zeta, and SEPIC are treated. It is also possible to apply it to quadratic converters and the d-square converter is taken as an example. A converter with a reduced duty cycle is also treated and a modification that avoids the inrush current is also shown. Finally, an improved superlift converter is treated. The position of the zero of the transfer function is exemplarily studied.

Key-Words: - DC/DC converter, tristate converter, Buck, Boost, Zeta, SEPIC, Cuk, quadratic, reduced duty cycle

Received: September 24, 2022. Revised: September 15, 2023. Accepted: Ocotber 17, 2023. Published: November 20, 2023.

1 Introduction

The starting point for this investigation is the paper, [1], where a tristate Boost converter with coupled coils is treated. The circuit behind this converter is published in, [2], [3], [4], and a controller design is treated in, [5]. A tristate Boost converter with a topology with little reduced forward-losses is treated in, [6], [7], and an extension with zero-voltage switching (ZVS) can be found in, [8]. Another ZVS concept is treated in, [9]. An interesting topology for an inverting tristate Buck-Boost converter is shown in, [10]. The basics of converters and many topologies are described in all the textbooks on Power Electronics, (e.g., [11], [12], [13]). It should be mentioned that other concepts exist to achieve tristate converters, [14]. The circuit diagram of the tristate Boost converter is shown in Figure 1.

In the continuous operation, the converter has three modes. The basic function is explained with ideal components (no parasitic resistors and infinite switching speed). In the first mode M1, both electronic switches S1 and S2 are on, the input voltage U1 is across the inductor L1, and the current increases. When S1 is turned off, the second mode M2 begins. Now diode D1 turns on and the inductor L1 is short-circuited. The current through the coil stays constant. When S2 is turned off, too, diode D2 turns on, and the difference between the input and the output voltages is across the inductor, and the current decreases.

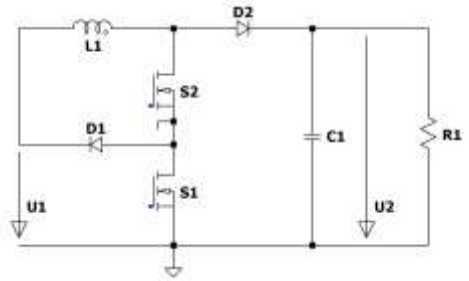

Fig. 1: Tristate Boost converter

The voltage-time balance in a steady state is therefore

$$U_1 d_1 T = |U_1 - U_2|(1-d_2)T \tag{1}$$

and the voltage transformation rate is achieved to

$$M = \frac{U_2}{U_1} = \frac{1+d_1-d_2}{1-d_2} \,. \tag{2}$$

Figure 2 shows the voltage transformation ratio for d_2 as a parameter and d_1 as the independent variable. The most interesting feature of this

converter is that the voltage transformation ratio is now linear for a constant duty cycle of switch S2. In the figure also the transformation ratio of the normal Boost converter is shown (the nonlinear line).

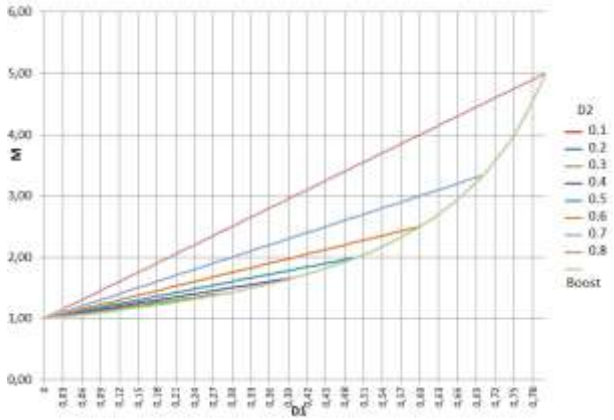

Fig. 2: Voltage transfer ratio for the tristate Boost converter: d_1 variable and d_2 as parameter

Figure 3 shows the voltage across the coil, the current through the inductor, the load current, the input and the output voltages, and the control signals of the switches in the steady state. All simulations are done with capacitor values of 330 µF and inductor values of 47 µH, an input voltage of 48 V, except when other values are given.

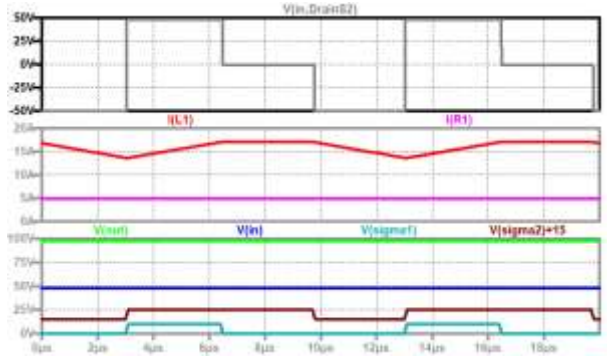

Fig. 3: Tristate Boost converter (up to down): voltage across coil L1 (grey); current through the inductor L1 (red), current through the load (violet); output voltage (green), input voltage (blue), a control signal for switch S2 (black, shifted), a control signal for switch S2 (turquoise)

2 Basic Tristate Converters

First, the other basic converters are changed into a tristate one.

2.1 Tristate Buck

The tristate Buck converter is shown in Figure 4. When both switches are on, the difference between the input voltage and the output voltage is across the inductor, and the current increases. When S1 turns off and S2 is still on, the current through the coil commutates into D1. The current stays nearly constant. When S2 is turned off too, the current commutates into the diode D2 and is free-wheeling. Now the negative output voltage is across the coil and the current decreases.

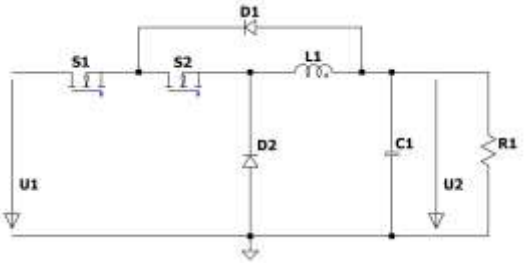

Fig. 4: Tristate Buck converter

The voltage-time balance can be written with the help of the duty cycles for both switches d_1 and d_2 (the duty cycle is defined by the on-time of the active switch referred to as the switching period) according to

$$(U_1 - U_2)d_1T = |-U_2|(1-d_2)T \tag{3}$$

leading to the voltage transformation ratio

$$M = \frac{U_2}{U_1} = \frac{d_1}{1+d_1-d_2} \ . \tag{4}$$

The connection between the load current and the mean value of the current through the coil can be found by the charge balance of the capacitor. With the mean value of the inductor current $\bar{I}_L$ one can write

$$(d_1+1-d_2)\left(\bar{I}_L - I_{LOAD}\right) = |-I_{LOAD}|(d_2-d_1) \, . \tag{5}$$

The mean value of the current through the coil is therefore

$$\bar{I}_L = \frac{I_{LOAD}}{1+d_1-d_2} \, . \tag{6}$$

Figure 5 shows the voltage across the coil, the current through the inductor, the load current, the input and the output voltages, and the control signals for the switches in the steady state.

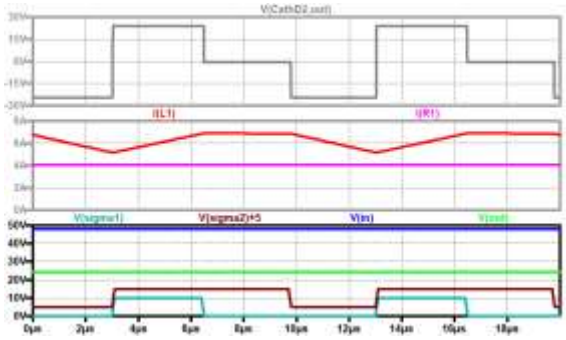

Fig. 5: Tristate Buck converter (up to down): voltage across the inductor L1 (grey); current through the inductor L1 (red), current through the load (violet); output voltage (green), input voltage (blue), a control signal for switch S2 (black, shifted), a control signal for switch S2 (turquoise)

Figure 6 shows the voltage transformation ratio for d2 as a parameter and d1 as the independent variable. The linear line corresponds to the normal Buck converter. The voltage transformation ratios for a constant duty cycle of the second switch are nonlinear.

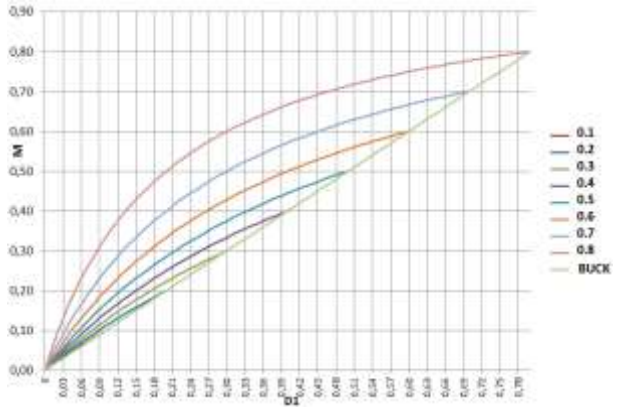

Fig. 6: Voltage transformation ratio for the tristate Buck converter d1 variable and d2 as parameter

2.2 Tristate Buck-Boost

Applying the tristate concept to the Buck-Boost converter leads to the circuit diagram Figure 7.

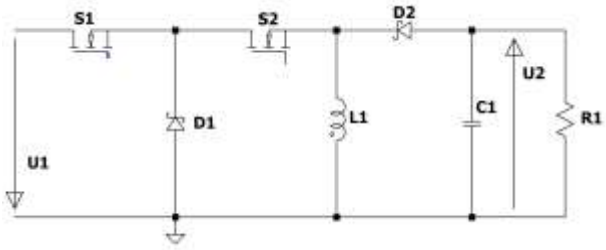

Fig. 7: Tristate Buck-Boost converter

When both switches (during the time interval $d_1 T$) are on, the input voltage is across the coil. When S1 is turned off and S2 is still on (during the time interval $(d_2 - d_1)T$), the inductor is short-circuited by S2 and D1 and the current stays nearly constant. When S2 is turned off, D2 turns on and the current free-wheels through D2. Now the negative output voltage is across the coil and the current decreases.

The voltage-time balance

$$U_1 d_1 T = |-U_2|(1-d_2)T \tag{7}$$

leads to the voltage transformation ratio

$$M = \frac{U_2}{U_1} = \frac{d_1}{1-d_2} . \tag{8}$$

Figure 8 shows the voltage across the coil, the current through the inductor, the load current, the input and the output voltages, and the control signals of the switches in the steady state.

Figure 9 shows the voltage transformation ratio for d2 as a parameter and d1 as the independent variable. The most interesting feature of this converter is that the voltage transformation ratio is now linear for a constant duty cycle of switch S2. In the figure also the transformation ratio of the normal Buck-Boost is shown (the nonlinear line).

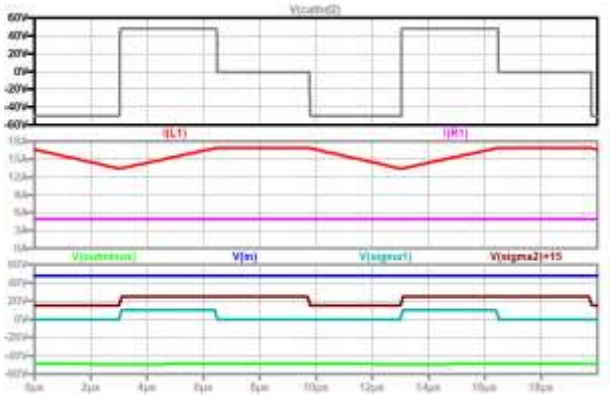

Fig. 8: Tristate Buck-Boost converter (up to down): voltage across the inductor L1 (grey); current through the inductor L1 (red), current through the load (violet); output voltage (green), input voltage (blue), control signal for switch S2 (black, shifted), control signal for switch S2 (turquoise)

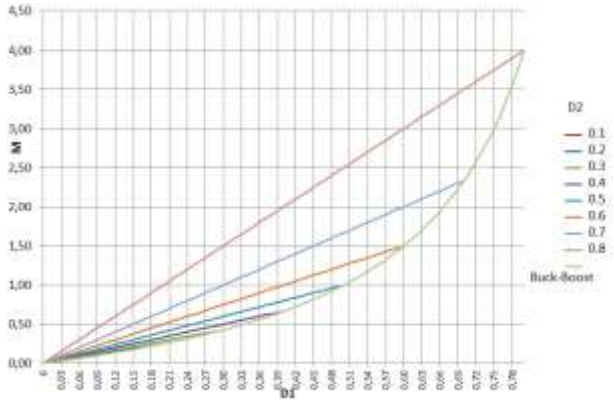

Fig. 9: Voltage transformation ratio for the tristate Buck-Boost converter with d1 variable and d2 as parameter

3 Higher order Tristate Converters

3.1 Tristate Zeta Converter

The circuit diagram of the tristate Zeta converter is shown in Figure 10. When both switches are on, the input voltage is across L1, when only S2 is on, a short-circuit of L1 occurs and the current stays nearly constant, and when S2 turns off too, the negative voltage across C1 is across the inductor and the current decreases. The voltage across C1 is equal to the output voltage during steady-state (the loop C1, L2, C2, L1 is always valid, and the mean value of the voltages across the coils must be zero).

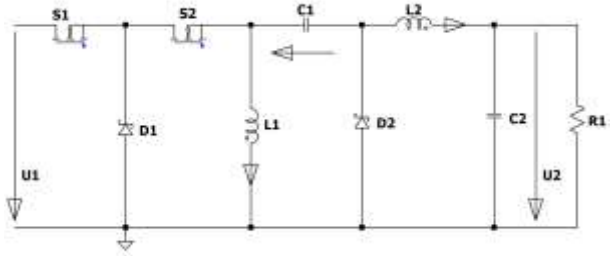

Fig. 10: Tristate Zeta converter

The voltage-time balance across L1 can be written according to

$$U_1 d_1 T = \left|-U_{C1}\right|(1-d_2)T \quad . \tag{9}$$

The voltage across C1 can be found by looking at the loop L1, C1, L2, C2 which is always valid to

$$U_{C1} = U_2 \tag{10}$$

leading again to the voltage transformation ratio of the Buck-Boost converter (Figure 9)

$$M = \frac{U_2}{U_1} = \frac{d_1}{1-d_2} \quad . \tag{11}$$

Figure 11 shows the voltage across the coil L1, the current through the inductors L1 and L2, the input and the output voltages, and the control signals for the switches in the steady state.

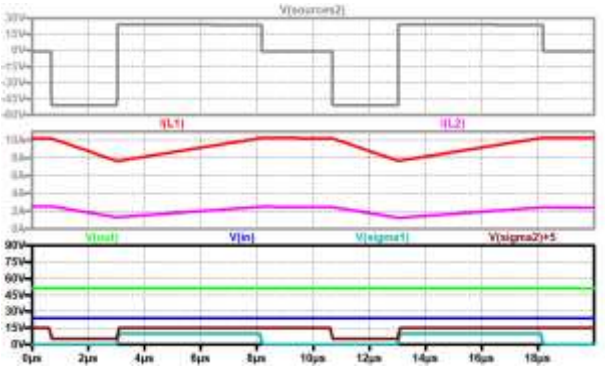

Fig. 11: Tristate ZETA converter (up to down): voltage across the inductor L1 (grey); current through the inductor L1 (red), current through the inductor L2 (violet); output voltage (green), input voltage (blue), a control signal for switch S2 (black, shifted), a control signal for switch S2 (turquoise)

3.2 Tristate Cuk Converter

In Figure 12 the circuit diagram of the Cuk converter which was transferred into a tristate one is shown. During the time interval, when both switches are on, the input voltage is across L1, and the current increases. When only S2 is on, the current through L1 is shunted by the diode D2 and the current stays nearly constant. When both switches are turned off, the current through L1 free-wheels through C1, D2, and back to the input source. Now the difference between the input voltage and the voltage across C1 is across the coil L1. The voltage across C1 is equal to the sum of the input and the output voltages.

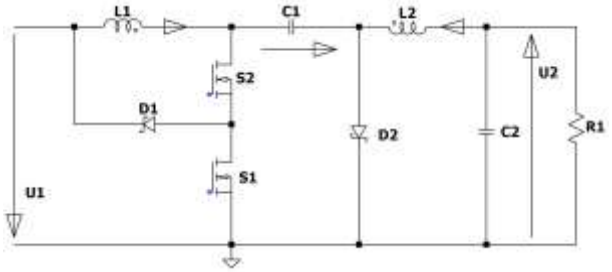

Fig. 12: Tristate Cuk converter

The voltage-time balance across L1 is therefore given according to

$$U_1 d_1 T = \left|U_1 - U_{C1}\right|(1-d_2)T \quad . \tag{12}$$

The voltage across C1 can be found by looking at the outer loop to

$$U_{C1} = U_1 + U_2 \tag{13}$$

leading again to the voltage transformation ratio of the Buck-Boost converter (Figure 9)

$$M = \frac{U_2}{U_1} = \frac{d_1}{1-d_2} . \quad (14)$$

Figure 13 shows the voltage across the coil L1, the current through the inductors L1 and L2, the input and the output voltages, and the control signals of the switches in the steady state.

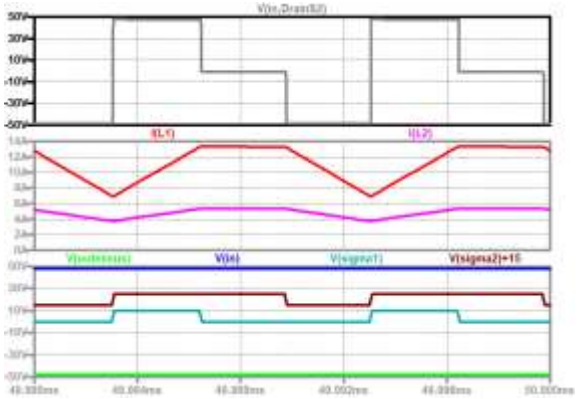

Fig. 13: Tristate CUK converter (up to down): voltage across the inductor L1 (grey); current through the inductor L1 (red), current through the inductor L2 (violet); output voltage (green), input voltage (blue), control signal for switch S2 (black, shifted), control signal for switch S1 (turquoise)

3.3 Tristate SEPIC Converter

The tristate Sepic converter is depicted in Figure 14. During the on-time of both switches the positive input voltage is across the inductor L1. This coil is short-circuited when S1 is turned off. When S2 is also turned off, the input voltage minus the sum of the voltages across the output and the capacitor C1 is across L1. Now one can write for the voltage-time balance across L1

$$U_1 d_1 = U_2 (1-d_2) \quad (15)$$

which leads to the voltage transformation ratio (equal to that of the Buck-Boost converter, Figure 9)

$$M = \frac{U_2}{U_1} = \frac{d_1}{1-d_2} . \quad (16)$$

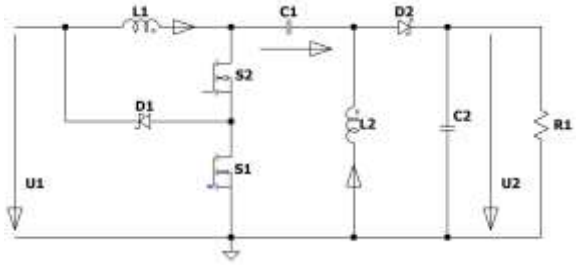

Fig. 14: Tristate Sepic converter

Figure 15 shows the voltage across the coil L1, the current through the inductors L1 and L2, the input and the output voltages, and the control signals for the switches in the steady state. The inductor values for this simulation are different from the ones that were used in the other simulations (L1=25 µH, L2=100 µH). Therefore, the current ripple through L1 is large.

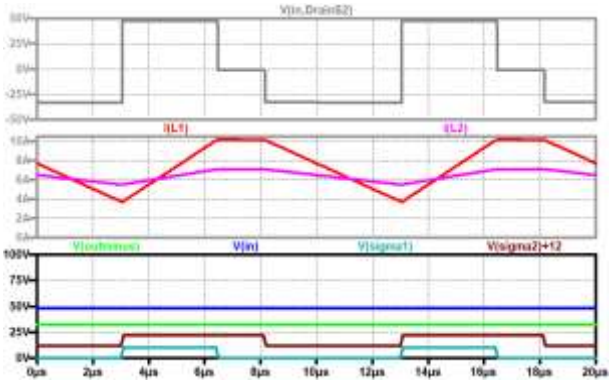

Fig. 15: Tristate Sepic converter with L1=25 µH and L2=100 µH (up to down): voltage across the inductor L1 (grey); current through the inductor L1 (red), current through the inductor L2 (violet); output voltage (green), input voltage (blue), a control signal for switch S2 (black, shifted), a control signal for switch S2 (turquoise)

3.4 Tristate D-Square Converter

The tristate D-square converter is shown in Figure 16. In its original topology, [15], this converter has only one switch and three diodes. The converter is especially useful for higher voltages and powers when IGBTs are used because diodes have a lower forward voltage than IGBTs. The voltage transformation ratio is the square of the duty cycle.

During M1 the input voltage minus the voltage across C1 is across L1 (when S1 and S2 are on, also D2 is on), during M2 the voltage is zero, and during the off-time of S2, the negative capacitor voltage of C1 is across L1. The voltage-time balance can be written according to

$$(U_1 - U_{C1}) d_1 = U_{C1} (1-d_2) . \quad 17)$$

The voltage across C1 can therefore be calculated according to

$$U_{C1} = \frac{d_1}{1+d_1-d_2} U_1 . \quad (18)$$

During M1 the voltage across L2 is the difference between the voltage across C1 and the output voltage U2. When S1 is off during M2 and

M3, the negative output voltage is across L2. The voltage-time balance is therefore

$$(U_{C1}-U_2)d_1 = U_2(1-d_1). \tag{19}$$

The output voltage can now be written by

$$U_2 = U_{C1}d_1. \tag{20}$$

The voltage transformation ratio can now be given according to

$$\frac{U_2}{U_1} = \frac{d_1^2}{1+d_1-d_2}. \tag{21}$$

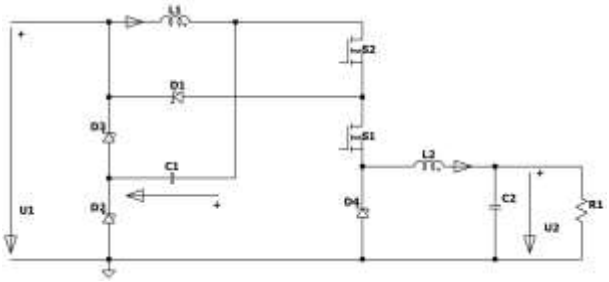

Fig. 16: Tristate d-square converter

Figure 17 shows the voltage transformation ratio for d2 as a parameter and d1 as independent variable. The quadratic line corresponds to the normal quadratic Buck converter. The voltage transformation ratios for a constant duty cycle of the second switch are slightly nonlinear.

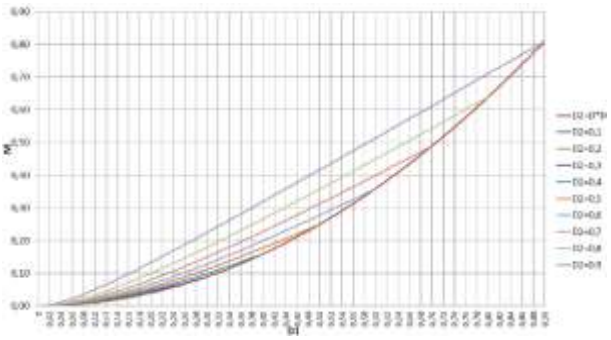

Fig. 17: Voltage transfer ratio for the tristate d-square converter, d1 variable and d2 as parameter

Figure 18 shows the voltage across the coil L1, the current through the inductors L1 and L2, the input and the output voltages, and the control signals for the switches in the steady state.

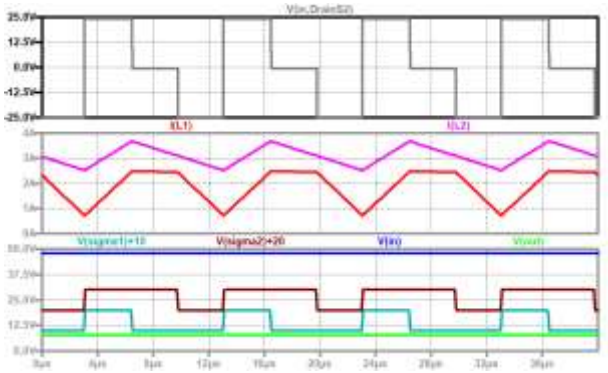

Fig. 18: Tristate d-square converter (up to down): voltage across the inductor L1 (grey); current through the inductor L1 (red), current through the inductor L2 (violet); input voltage (blue), a control signal for switch S2 (black, shifted), a control signal for switch S2 (turquoise), output voltage (green)

3.5 Tristate (2d-1)/(1-d) Converter

This is a very special converter type and the circuit diagram is depicted in Figure 19.

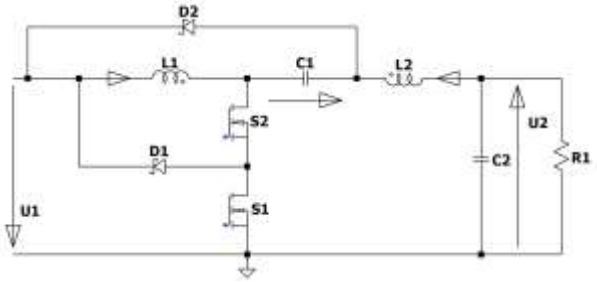

Fig. 19: Tristate (2d-1)/(1-d) converter

Again the converter has three modes. During mode M1 both electronic switches S1 and S2 are on, and the input voltage is across the first coil L1. Mode M2 starts when S1 is turned off and is an idling mode. The current through L1 stays constant because now the coil L1 is short-circuited by the diode D1 and the electronic switch S2. When S2 is turned off, D2 turns on and the negative voltage of the capacitor C1 is across the coil L1, and the current through it decreases. The voltage-time balance is therefore

$$U_1 d_1 T = |U_C|(1-d_2)T = |-U_1-U_2|(1-d_2)T \tag{22}$$

leading to

$$M = \frac{U_2}{U_1} = \frac{d_1+d_2-1}{1-d_2}. \tag{23}$$

A very interesting aspect of this converter is that compared to the original converter which has the voltage transformation ratio

$$M = \frac{U_2}{U_1} = \frac{2d-1}{1-d} \tag{24}$$

which reduces the duty cycle to a value greater than 0.5, now lower duty cycles are possible, depending on the duty cycle of switch S2.

Figure 20 shows the voltage transformation ratio for d2 as a parameter and d1 as the independent variable. The most interesting feature of this converter is that the voltage transformation ratio is now linear for a constant duty cycle of switch S2. In the figure, the transformation ratio of the normal (2d-1)/(1-d) converter is shown (the nonlinear line). The graphs are only valid for M greater than zero. So one can see that for d2 of 90 % a d1 of greater than 10 % is possible, or for d2=0.8 a d1 greater than 20 % can be used.

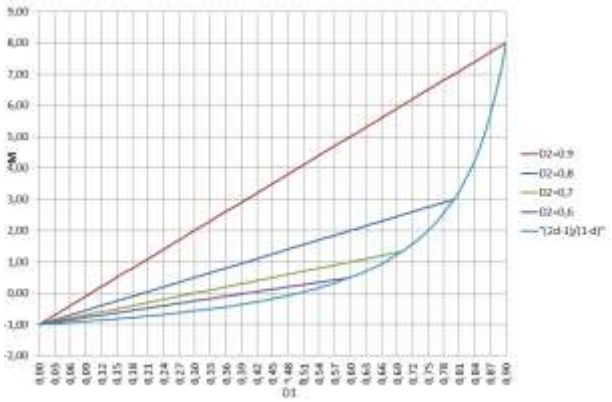

Fig. 20: Voltage transformation ratio for the tristate (2d-1)/(1-d) converter: d1 variable and d2 as parameter

Figure 21 shows the voltage across the coil L1, the current through the inductors L1 and L2, the input and the output voltages, and the control signals of the switches in the steady state for a combination of duty cycles greater than 50 % (60 % and 80 %). Figure 22 shows the same signals for d1=33 % and d2=80 %.

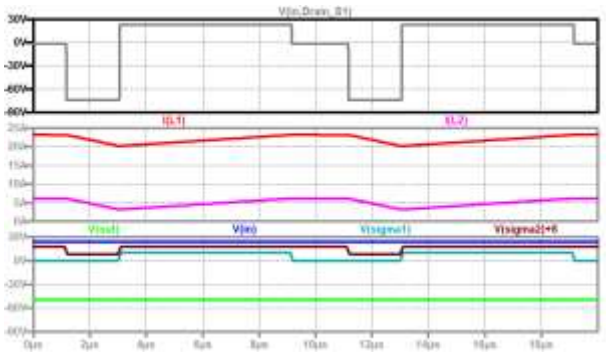

Fig. 21: Tristate (2d-1)/(1-d) converter with U1=24 V, d1=60 % and d2=80 % (up to down): voltage across the inductor L1 (grey); current through the inductor L1 (red), current through the inductor L2 (violet); input voltage (blue), control signal for switch S2 (black), control signal for switch S2 (turquoise), output voltage (green)

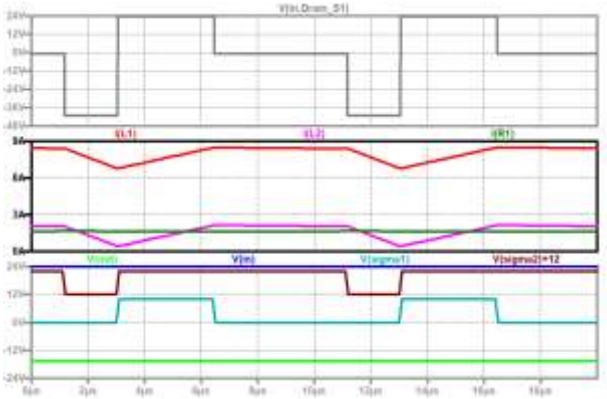

Fig. 22: Tristate (2d-1)/(1-d) converter with U1=24 V, d1=33 % and d2=80 % (up to down): voltage across L1 (grey); current through L1 (red), current through L2 (violet); load current (brown); input voltage (blue), control signal for S2 (black, shifted), control signal for S1 (turquoise), output voltage (green)

Another interesting and important aspect of converters is the inrush current when the converter is applied to a stable input voltage. Figure 23 shows the inrush of the converter. A damped ringing with high amplitude at the beginning occurs. The output voltage is positive at the beginning (the converter is an inverting one) and not negative during the inrush. This can be dangerous for the applied load.

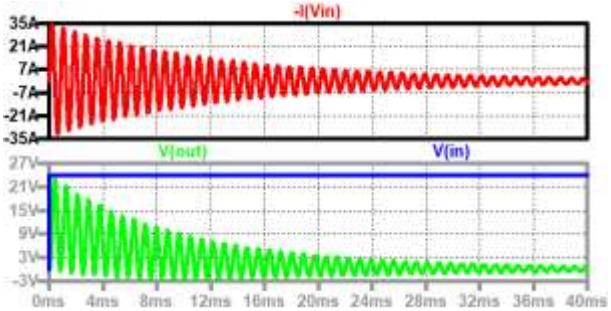

Fig. 23: Tristate (2d-1)/(1-d) converter inrush, up to down: input current (red); input voltage (blue), output voltage (green)

To avoid the inrush, a small modification of the converter has to be done, as shown in the next paragraph.

3.6 Tristate (2d-1)/(1-d) Converter Type 2A

The basic converter topology is shown in, [16], and the tristate version is given in Figure 24. Other

modified converters with reduced duty cycle are presented in, [17], and can also be transformed into tristate ones. Figure 25 shows the inrush into this converter. The modification of the position of the second capacitor avoids a large inrush current which stresses all components. The voltage transformation ratio is shown in Figure 20.

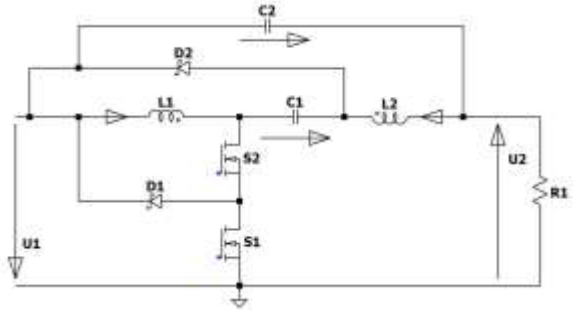

Fig. 24: Modified tristate (2d-1)/(1-d) converter type 2A

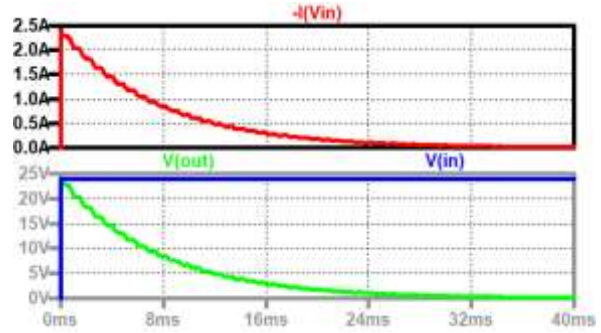

Fig. 25: Tristate (2d-1)/(1-d) converter type 2A, inrush (up to down): input current (red); input voltage (blue), output voltage (green)

Figure 26 shows the voltage across the coil L1, the current through the inductors L1 and L2, the input and the output voltages, and the control signals for the switches in the steady state for a combination of duty cycles greater than 50 %.

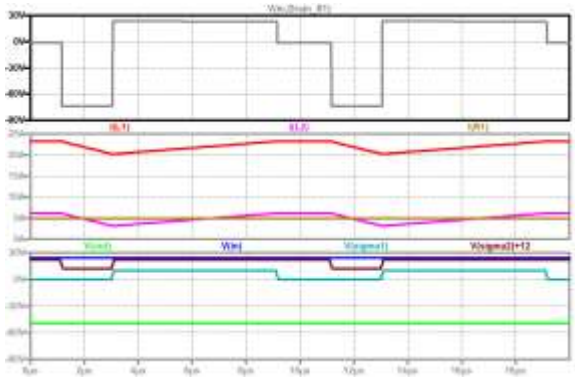

Fig. 26: Tristate (2d-1)/(1-d) converter type 2A, (up to down): voltage across L1 (grey); current through L1 (red), current through L2 (violet); load current (brown); input voltage (blue), control signal for S2 (black, shifted), control signal for S1 (turquoise), output voltage (green)

3.7 Tristate Improved Superlift Converter

Superlift converters, [18], are another interesting topology. The original converter, [19], has large peaks in the input current. This can be avoided when a small inductor L2 is placed in series to the diode D1, [20]. The circuit diagram can be seen in Figure 27. When both electronic switches are on in mode M1, the capacitor C1 is charged and during M3 the voltage across the capacitor C1 decreases. In the mean, the voltage across C1 must be equal to the input voltage U1.

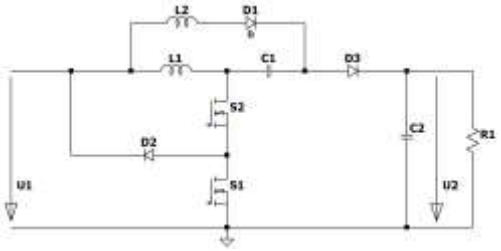

Fig. 27: Improved positive output super-lift Boost converter

During M1 U1 is across the inductor, during M2 the voltage across it is zero, and during M3 the input voltage plus the voltage across C1 minus the output voltage is across the coil L1. The voltage-time balance is therefore

$$U_1 d_1 = |2U_1 - U_2|(1-d_2) \tag{25}$$

leading to

$$M = \frac{U_2}{U_1} = \frac{2+d_1-2d_2}{1-d_2}. \tag{26}$$

Figure 28 shows the voltage transformation ratio for d2 as a parameter and d1 as the independent variable. Again the curves are linearized.

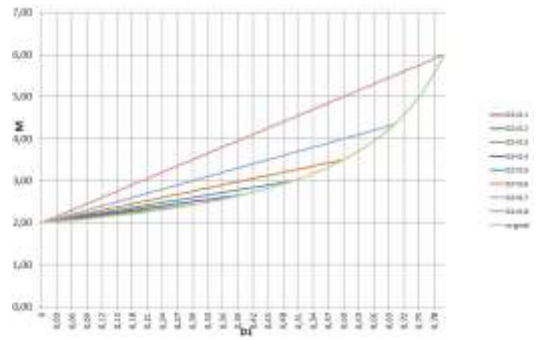

Fig. 28: Voltage transformation ratio for the tristate improved positive output super-lift Boost converter: d1 variable and d2 as parameter

Figure 29 shows the voltage across the coil L1, the current through the inductors L1 and L2, the input and the output voltages, and the control signals for the switches in the steady state. Also, the current through the inductor L2 which charges the capacitor C1 is depicted.

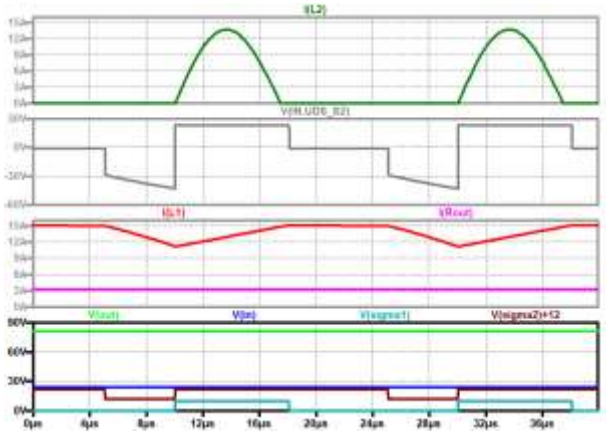

Fig. 29: Improved positive output super-lift Boost converter, (up to down): current through L2 (dark green); voltage across L1 (grey); current through L1 (red), current through L2 (violet); load current (brown); input voltage (blue), control signal for S2 (black, shifted), control signal for S1 (turquoise), output voltage (green)

4 Position of the Zero

Converters with the possibility to increase the output voltage over the input voltage, like the Boost, Buck-Boost, Cuk, Sepic, etc. are non-phase-minimum systems, which means they have a zero on the right side of the complex plane RHZ (right half-plane zero). RHZs influence the phase and lead to further negative phase shifts. To stabilize the control, a lower crossover frequency is necessary and the whole system gets slower.

To calculate the zero, a linear dynamic model must be derived and the transfer functions ascertained. This is shown now for the tristate Buck-Boost converter. The state equation during M1 are

$$\frac{di_{L1}}{dt}=\frac{u_1}{L_1} \qquad \frac{du_{C1}}{dt}=\frac{-u_{C1}/R_1}{C_1}, \tag{27}$$

during M2

$$\frac{di_{L1}}{dt}=\frac{0}{L_1} \qquad \frac{du_{C1}}{dt}=\frac{-u_{C1}/R_1}{C_1}, \tag{28}$$

and during M3

$$\frac{di_{L1}}{dt}=-\frac{u_{C1}}{L_1} \qquad \frac{du_{C1}}{dt}=\frac{i_{L1}-u_{C1}/R_1}{C_1}. \tag{29}$$

Mode M1 must be weighted by d1, mode M3 must be weighted by (1-d2) and the discharge of the capacitor by the load current is valid all the time. This leads to the large signal model

$$\frac{d}{dt}\begin{pmatrix} i_{L1} \\ u_{C1} \end{pmatrix}=\begin{bmatrix} 0 & \frac{d_2-1}{L_1} \\ \frac{1-d_2}{C_1} & -\frac{1}{RC_1} \end{bmatrix}\begin{pmatrix} i_{L1} \\ u_{C1} \end{pmatrix}+\begin{bmatrix} \frac{d_1}{L_1} \\ 0 \end{bmatrix}(u_1) \ . \tag{30}$$

To get transfer functions of the converter for drawing Bode plots and to design controllers, (30) has to be linearized by the perturbation ansatz. The variables are written as the operating point value, written with a capital letter and a zero in the index, plus a small disturbance, written with small letters with a roof on top. Linearization leads to

$$\frac{d}{dt}\begin{pmatrix} \hat{i}_{L1} \\ \hat{u}_{C1} \end{pmatrix}=\begin{bmatrix} 0 & \frac{D_{20}-1}{L_1} \\ \frac{1-D_{20}}{C_1} & -\frac{1}{RC_1} \end{bmatrix}\begin{pmatrix} \hat{i}_{L1} \\ \hat{u}_{C1} \end{pmatrix}+ \begin{bmatrix} \frac{D_{10}}{L_1} & \frac{U_{10}}{L_1} & \frac{U_{C10}}{L_1} \\ 0 & 0 & -\frac{I_{L10}}{C_1} \end{bmatrix}\begin{pmatrix} \hat{u}_1 \\ \hat{d}_1 \\ \hat{d}_2 \end{pmatrix}. \tag{31}$$

With abbreviations, one can write (32)

$$\frac{d}{dt}\begin{pmatrix} \hat{i}_{L1} \\ \hat{u}_{C1} \end{pmatrix}=\begin{bmatrix} 0 & A_{12} \\ A_{21} & A_{22} \end{bmatrix}\begin{pmatrix} \hat{i}_{L1} \\ \hat{u}_{C1} \end{pmatrix}+\begin{bmatrix} B_{11} & B_{12} & B_{13} \\ 0 & 0 & B_{23} \end{bmatrix}\begin{pmatrix} \hat{u}_1 \\ \hat{d}_1 \\ \hat{d}_2 \end{pmatrix}.$$

Laplace transformation leads to (33)

$$\begin{bmatrix} s & -A_{12} \\ -A_{21} & s-A_{22} \end{bmatrix}\begin{pmatrix} I_{L1}(s) \\ U_{C1}(s) \end{pmatrix}=\begin{bmatrix} B_{11} & B_{12} & B_{13} \\ 0 & 0 & B_{23} \end{bmatrix}\begin{pmatrix} U_1(s) \\ D_1(s) \\ D_2(s) \end{pmatrix}.$$

The denominator is the same for all transfer functions

$$Den=s^2-A_{22}s-A_{12}A_{21} \ . \tag{34}$$

The numerator of the transfer function between capacitor (output) voltage and the duty cycle of switch S1 can be calculated according to

$$NumUC1D1=\begin{vmatrix} s & B_{12} \\ -A_{21} & 0 \end{vmatrix}=A_{21}B_{12} \ . \tag{35}$$

The transfer function has no zero and describes a phase-minimum system.

The numerator of the transfer function between capacitor (output) voltage and the duty cycle of switch S2

$$NumUC1D2 = \begin{vmatrix} s & B_{13} \\ -A_{21} & B_{23} \end{vmatrix} = sB_{23} + A_{21}B_{13} \quad (36)$$

has a zero on the right half-plane, because B_{23} is negative. This transfer function describes a non-phase-minimum system.

The conclusion is therefore: one has to control the duty cycle of switch S1 and use a constant duty cycle of switch S2.

As a second example, the modified tristate (2d-1)/(1-d) converter Type 2A is used. In the same way, as shown before the small signal model is derived according to

$$\frac{d}{dt}\begin{pmatrix} \hat{i}_{L1} \\ \hat{i}_{L2} \\ \hat{u}_{C1} \\ \hat{u}_{C2} \end{pmatrix} = \begin{bmatrix} 0 & 0 & \frac{D_{20}-1}{L_1} & 0 \\ 0 & 0 & \frac{D_{20}}{L_2} & -\frac{1}{L_2} \\ \frac{1-D_{20}}{C_1} & -\frac{D_{20}}{C_1} & 0 & 0 \\ 0 & \frac{1}{C_2} & 0 & -\frac{1}{RC_2} \end{bmatrix} \begin{pmatrix} \hat{i}_{L1} \\ \hat{i}_{L2} \\ \hat{u}_{C1} \\ \hat{u}_{C2} \end{pmatrix} + \begin{bmatrix} \frac{D_{10}}{L_1} & \frac{U_{10}}{L_1} & \frac{U_{C10}}{L_1} \\ 0 & 0 & \frac{U_{C10}}{L_2} \\ 0 & 0 & -\frac{I_{L10}}{C_1} \\ \frac{1}{RC_2} & 0 & 0 \end{bmatrix} \begin{pmatrix} \hat{u}_1 \\ \hat{d}_1 \\ \hat{d}_2 \end{pmatrix} \quad (37)$$

This results again in a numerator for the transfer function between the voltage across C2 and the duty cycle d1

$$NumUC2D1 = A_{23}A_{31}A_{42}B_{12} \quad (38)$$

which has no zero and therefore results in a phase minimum system.

5 Conclusion

Tri-state converters, achieved by the method used here, have some very interesting features:

- An additional degree of freedom in the voltage transformation ratio
- Linearized voltage transformation ratio for converters with step-up capability
- Phase minimum system for constant duty cycle of the second switch for converters with step-up possibility

The concept can be used for many other DC/DC converter topologies.

References:

[1] G M. A. Vaghela and M. A. Mulla, Tri-State Coupled Inductor Based High Step-Up Gain Converter Without Right Hand Plane Zero, *IEEE Transactions on Circuits and Systems II: Express Briefs*, vol. 70, no. 6, pp. 2291-2295, June 2023, doi: 10.1109/TCSII.2023.3237679.

[2] K. Viswanathan, R. Oruganti and D. Srinivasan, Dual-mode control of tri-state boost converter for improved performance, *IEEE Transactions on Power Electronics*, vol. 20, no. 4, pp. 790-797, July 2005, doi: 10.1109/TPEL.2005.850907.

[3] K. Viswanathan, R. Oruganti and D. Srinivasan, A novel tri-state boost converter with fast dynamics, *IEEE Transactions on Power Electronics*, vol. 17, no. 5, pp. 677-683, Sept. 2002, doi: 10.1109/TPEL.2002.802197.

[4] S. K. Viswanathan, R. Oruganti and D. Srinivasan, Dual mode control of tri-state boost converter for improved performance, *IEEE 34th Annual Conference on Power Electronics Specialist*, Acapulco, Mexico, 2003, pp. 944-950 vol.2, doi: 10.1109/PESC.2003.1218182.

[5] S. Sarkar, A. Ghosh and S. Banerjee, Design and implementation of type-III controller in tri state boost converter, *2015 Annual IEEE India Conference (INDICON)*, New Delhi, India, 2015, pp. 1-6, doi: 10.1109/INDICON.2015.7443152.

[6] K. Viswanathan, R. Oruganti and D. Srinivasan, Tri-state boost converter with no right half plane zero, *4th IEEE International Conference on Power Electronics and Drive Systems*. IEEE PEDS 2001 - Indonesia. Proceedings (Cat. No.01TH8594), Denpasar, Indonesia, 2001, pp. 687-693 vol.2.

[7] S. Kapat, A. Patra and S. Banerjee, A novel current controlled tri-state boost converter with superior dynamic performance, *2008 IEEE International Symposium on Circuits and Systems*, Seattle, WA, USA, 2008, pp. 2194-2197.

[8] K. Kumar, N. Rana, S. Banerjee, S. B. Santra and N. Parvez, Design and analysis of soft-switched tri-state boost converter, 2018 International *Conference on Power, Instrumentation, Control and Computing (PICC)*, Thrissur, India, 2018, pp. 1-6.

[9] O. Knecht, D. Bortis and J. W. Kolar, ZVS Modulation Scheme for Reduced Complexity Clamp-Switch TCM DC–DC Boost

Converter, *IEEE Transactions on Power Electronics*, vol. 33, no. 5, May 2018, pp. 4204-4214.

[10] N. Rana and S. Banerjee, Interleaved Tri-state Buck-Boost Converter with Fast Transient Response and Lower Ripple, *2019 IEEE Transportation Electrification Conference (ITEC-India)*, Bengaluru, India, 2019, pp. 1-5.

[11] N. Mohan, T. Undeland and W. Robbins, *Power Electronics, Converters, Applications and Design*, 3nd ed. New York: W. P. John Wiley & Sons, 2003.

[12] F. Zach, *Power Electronics*, in German: Leistungselektronik, Frankfurt: Springer, 6th ed., 2022.

[13] Y. Rozanov, S. Ryvkin, E. Chaplygin, P. Voronin, *Power Electronics Basics*, CRC Press, 2016.

[14] F. A Himmelstoss, Concept to change the voltage transformation ratio of a DC/DC converter, *Cukurova 9th International Scientific Researches Conference*, Adana, Turkey, October 9-11, 2022, pp. 258-273, ISBN: 978-625-8246-28-5.

[15] D. Maksimovic, and S. Cuk: Switching converters with wide DC conversion range, *IEEE Transactions on Power Electronics*, vol. 6, January 1991, pp. 151 – 157.

[16] F. A. Himmelstoss, and M. Jungmayer, A Family of Modified Converters with Limited Duty Cycle, 2021 *International Aegean Conference on Electrical Machines and Power Electronics (ACEMP) & 2021 International Conference on Optimization of Electrical and Electronic Equipment (OPTIM)*, Brasov, Romania, 2021, pp.246-253.

[17] F. A. Himmelstoss, and K. H. Edelmoser, A Topology to generate DC/DC, AC/DC, DC/AC, and AC/AC Converters, *2021 25th International Conference on Circuits, Systems, Communications and Computers (CSCC)*, 2021 pp. 102-110.

[18] Fang Lin Luo, Six self-lift DC-DC converters, voltage lift technique, *IEEE Transactions on Industrial Electronics*, vol. 48, no. 6, Dec. 2001, pp. 1268-1272.

[19] Fang Lin Luo and Hong Ye, Positive output super-lift converters, *IEEE Transactions on Power Electronics*, vol. 18, no. 1, Jan. 2003, pp. 105-113.

[20] F. A. Himmelstoss, Improved positive output voltage super-lift Boost converter, *WSEAS Transactions on Power Systems*, Vol. 17, 2022, E-ISSN: 2224-350X, pp. 68-75. https://doi.org/10.37394/232016.2022.17.8

Contribution of Individual Authors to the Creation of a Scientific Article (Ghostwriting Policy)

The author contributed in the present research, at all stages from the formulation of the problem to the final findings and solution.

Sources of Funding for Research Presented in a Scientific Article or Scientific Article Itself

No funding was received for conducting this study.

Conflict of Interest

The author has no conflicts of interest to declare.